Efficient Simulation Method for DFB Lasers with Large Gain Saturation Effect

Yanping Xi[1], *Member, IEEE,* Lin Han[2], Xun Li[2], *Senior Member, IEEE*
[1]Wuhan Nantional Laboratory for Optoelectronics, Huazhong Universtiy of Science and Technology
Wuhan, Hubei, China 430074
[2]Department of Electrical & Computer Engineering, McMaster University,
Hamilton, Ontario, Canada   L8S 4K1

Abstract—**In this paper, we proposed a nonlinear approximation scheme to the time-dependent longitudinal carrier distribution with a view toward finding the efficient solution scheme of the previously proposed standing-wave model for simulation of DFB lasers. It shows its advantage over the existing linear approximation scheme in cases where the optical power is large enough to trigger the saturation effect. The validity of this improved scheme is demonstrated by simulation example of $\lambda/4$-shifted DFB lasers.**

I. INTRODUCTION

In the description of DFB lasers, the accurate analysis of the longitudinal spatial hole burning (LSHB) effect is thought to be indispensible[1]. Several longitudinal one-dimensional models have been reported with the complex LSHB effect included[2-5]. The standing-wave model (SWM-CCM) in [5], utilizes the mode expansion technique to avoid the spatial discretization of the optical field, and consequently shows its higher efficiency in modeling DFB lasers. By linearly linking the shape of the longitudinal optical field to that of the carrier, Kinoshita[6] proposed an idea to "globally" approximate the carrier distribution with only two scalar quantities: one measures the average; the other represents the inhomogeneity of the distribution. A significant improvement of the computational efficiency of the SWM was also achieved by using this splitting idea[7]. However, the inhomogeneous part of the carrier distribution is assumed to linearly change with that of the optical field distribution in [6,7], which is not valid when the nonlinear gain saturation effect is large. To remedy this problem, we propose in this paper a nonlinear approximation to the carrier distribution for describing the large nonlinear interaction between the optical field and the carrier density distributions.

II. THEORY

The time-dependent carrier densities at different longitudinal positions are normally solved by the carrier rate equation

$$\frac{dN(z,t)}{dt} = \frac{I}{eV} - \frac{N(z,t)}{\tau_c} - \upsilon_g \Gamma g(z,t) P(z,t) \qquad (1)$$

where I the injected current, V the active region volume of the laser diode, e the electron charge, τ_c effective carrier life time and $P(z,t)$ the photon density distribution. For the SWM in [6], the carrier density evolution at different position inside the laser cavity is still obtained by discretizing the cavity into a number of spatial segments. Considering that the longitudinal carrier distribution normally has an opposite pattern from that of the photon distribution, $N(z,t)$ is linearly approximated by a deviation shape function $f(z,t)$ extracted from $P(z,t)$ in [7] to reduce the complexity of the existing SWM, i.e. if we define the time-dependent average photon density along the laser cavity as

$P_{av}(t)$, the photon density distribution can be expressed by

$$P(z,t) = P_{av}(t)\left[1 + f(z,t)\right], \text{ with } \int_0^L f(z,t)\,dz = 0. \text{ The carrier}$$

distribution can then be approximated by

$$N(z,t) = N_a(t) - D(t) f(z,t). \qquad (2)$$

where $N_a(t)$ and $D(t)$ measure the average and the inhomogeneity of the distribution, respectively. Equation (2) is valid by assuming the moderate optical power inside the cavity, therefore is no longer an appropriate approximation for the DFB laser if nonlinear saturation starts to kick on. In such cases, the carrier profile should be modeled by a nonlinear relationship in terms of the shape function $f(z,t)$. We thus proposed the following approximation to the carrier density distribution

$$N(z,t) = \frac{x(t)}{1 + f(z,t)} - \frac{y(t)}{\left[1 + f(z,t)\right]^2} + N_0. \qquad (3)$$

The function $f(z,t)$ indicates the carrier non-uniformity and is determined mainly by parameters of the laser structure such as κL and facet reflectivities, and hence it is reasonable to take $f(z,t)$ to be slowly varying compared with time-dependent coefficient $x(t)$ and $y(t)$. As such, when (3) is applied, Equation (1) is reduced to

$$\frac{dx(t)}{dt} = \left(\frac{I}{eV} - \frac{N_0}{\tau_c}\right)\left(2 + \frac{\theta_3}{\theta_2}\right) - \frac{x(t)}{\tau_c}$$
$$-\upsilon_g \frac{\Gamma g_N P_{av}(t)}{1 + \varepsilon P_{av}(t)}\left[\left(2 + \frac{\theta_3}{\theta_2}\right)x(t) - y(t)\right] \qquad (4)$$

$$\frac{dy(t)}{dt} = \left(\frac{N_0}{\tau_c} - \frac{I}{eV}\right)\frac{\theta_2}{\theta_f} - \frac{y(t)}{\tau_c} + \upsilon_g \frac{\Gamma g_N P_{av}(t)}{1 + \varepsilon P_{av}(t)}\left[\frac{\theta_2}{\theta_f}x(t)\right], \qquad (5)$$

where $\theta_2 = \frac{1}{L}\int_0^L f^2\,dz$, $\theta_3 = \frac{1}{L}\int_0^L f^3\,dz$, $\theta_4 = \frac{1}{L}\int_0^L f^4\,dz$ and $\theta_f = \frac{1}{L}\int_0^L \frac{f}{f+1}dz$. Along with the governing equation for the complex amplitude of each longitudinal mode in the SWM[6], i.e.

$$\frac{d\mathbf{A}_m(t)}{dt} = p'_{mm}(t)\mathbf{A}_m(t) + \sum_{n=1(n\neq m)}^{K} p'_{mn}(t)\mathbf{A}_n(t) + \tilde{\eta}_m(t), \text{ m=1,2,..K,} \qquad (6)$$

the DFB laser can be simulated in a selfconsistent manner. K is the number of eigenmodes used in the field expansion. More details of (6) can be found in [5,7].

III. SIMULATION RESULTS

In a λ/4-shifted DFB laser, the carrier profile becomes highly non-uniform due to the severe LSHB effects in the presence of strong coupling strength and relatively high injection level, and is thus chosen to be the simulation example.

The SWM-CCM without the carrier approximation is treated as our benchmark and denoted as Scheme I. The SWM-CCM with linear carrier approximation [8] is denoted as Scheme II and the proposed one with nonlinear carrier approximation is designated as Scheme III.

we define the error of the carrier distribution as

$$\varepsilon_N = \left(\sqrt{\sum_{z_i \in [0,L]} \left| \tilde{N}(z_i) - \hat{N}(z_i) \right|^2} \Big/ \sqrt{\sum_{z_i \in [0,L]} \left| \hat{N}(z_i) \right|^2} \right) \times 100\% \quad , \text{where} \quad \tilde{N}(z_i)$$

denotes the approximated carrier distribution obtained by scheme II or III, and $\hat{N}(z_i)$ represents the benchmark calculated by scheme I. Fig. 3 plots the change of ε_N with the bias level for different normalized coupling coefficients. As is expected, the simulation results show that the proposed scheme III gives a more accurate description of the carrier distribution than scheme II when the bias exceeds certain critical level, where the nonlinear saturation starts to take effect. With the increase of the coupling strength, the range of the injection level where the scheme III prevails is increasing. And the improvement of the accuracy is more pronouncing for lasers with large κL, i.e. with more severe nonlinear saturation effects.

One of the most important characteristics of the later is the output power obtained at the laser facets. Since both of the facets of the structure under investigation are AR-coated, the steady-state output power in our simulation is extracted at one end when the transient settles down. The error of the output power is defined as $\varepsilon_P = \left| \left(P_{II(\text{ or } III)} - P_I \right) / P_I \right| \times 100\%$, where P_I, P_{II} and P_{III} denote the output power obtained by scheme I, II and III, respectively. The change of this error with the coupling strength for a given bias is shown in Fig. 4. Similar performances are observed around $\kappa L = 1.25$, while scheme III outperforms scheme II when the normalized coupling strength is away from this value. This is due to the fact that the optical field is relatively uniform when $\kappa L = 1.25$, and becomes non-uniform enough to jeopardize the assumption of the linear approximation when the peaks of the optical field reach the saturation level for the laser with undercoupling or overcoupling.

The proposed scheme is of equal importance and can be viewed as a complementary scheme to scheme II. The detailed comparisons of computation complexity between three schemes are listed in Table I.

IV. SUMMARY

This paper presents an approximation to the carrier distribution which is nonlinearly related to the photon density profile. The proposed scheme is demonstrated to be effective in simulating DFB lasers with large saturation effects through comparing with the benchmark scheme as well as the existing linearly approximated scheme.

References:

[1] J. E. A. Whiteaway, B. Garretty, G. H. B. Thompson, A. J. Collar, C. J. Armistead and M. J. Fice, *IEEE J. Quantum Electron.* 28 (1992) 1277.

[2] P. Vankwikelberge, G. Morthier, and R. Baets, *IEEE J. Quantum Electron.* 26 (1990) 1728.

[3] B. -S. Kim, Y. Chung, and J. –S. Lee, *IEEE J. Quantum Electron.* 36 (2000) 787.

[4] H. Wenzel, U. Bandelow, H. -J. Wünsche, and J. Rehberg, *IEEE J. Quantum Electron.* 32(1996) 69.

[5] Y. Xi, X. Li and W. -P. Huang, *IEEE J. Quantum Electron.* 44 (2008) 931.

[6] J. Kinoshita and K. Matsumoto, *IEEE J. Quantum Electron.* 24 (1988) 2160.

[7] Y. Xi, W. –P. Huang and X. Li, *IEEE/OSA J. Lightwave Tech.* 27 (2009) 3227.
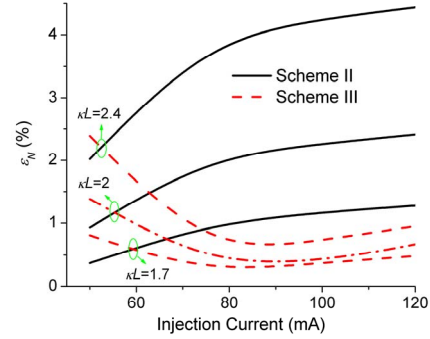
Fig.1 Variations of the error of carrier distributions with injection level for structures with different normalized coupling coefficients
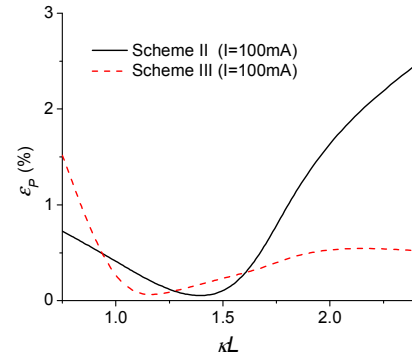

Fig.2 Variations of the error of the output power with normalized coupling coefficients for scheme II and III

TABLE I

COMPARSONS OF SCHEME I, II AND III

	Optical field		Carrier density		Total # of ODEs	Scope of Applications
	Discret-ization	# of ODEs	Discret-ization	# of ODEs		
Scheme I	no	K	yes	M	$K+M$	General
Scheme II	no	K	no	2	$K+2$	Small to moderate nonlinear saturation
Scheme III	no	K	no	2	$K+2$	Moderate to large nonlinear saturation

M: The number of sub-sections divided along the laser cavity (normally in several tenths for cavity length of several hundred micrometers).

K: The number of eigenmodes used in the field expansion.